DOI: 10.1021/ma100479x

Macromolecules
ARTICLE

Surface-Initiated Ring-Opening Metathesis Polymerization of Pentadecafluorooctyl-5-norbornene-2-carboxylate from Variable Substrates Modified with Sticky Biomimic Initiator

Qian Ye,[†,‡] Xiaolong Wang,[†] Shaobai Li,[‡] and Feng Zhou*[,†]

[†]*State Key Laboratory of Solid Lubrication, Lanzhou Institute of Chemical Physics, Chinese Academy of Sciences, Lanzhou 730000, China, and* [‡]*State Key Laboratory of Applied Organic Chemistry, College of Chemistry and Chemical Engineering, Lanzhou University, Lanzhou 730000, China*

Received March 2, 2010; Revised Manuscript Received May 24, 2010

ABSTRACT: A novel strategy is reported to produce low surface energy poly(pentadecafluorooctyl-5-norbornene-2-carboxylate) brushes (PNCA-F_{15}) on surfaces of variable metals and metallic oxides. PNCA-F_{15} brushes are grafted from biomimic catecholic initiator via surface-initiated ring-opening metathesis polymerization at ambient conditions. The biomimic catecholic initiator can assemble on a variety of substrates, such as Ti(TiO_2), Al(Al_2O_3), steel, Au, Cu, Ag, and Zn, and on both nanoparticles and planar substrates, allowing successful grafting of low surface energy polymer brushes from these substrates. The polymer brush modified substances were characterized by thermogravimetric analysis, X-ray photoelectron spectroscopy, water contact angle measurements, and atomic force microscopy. The PNCA-F_{15} brushes grow progressly with time with highly uniform surface coverage. Very uniform polymer layer with the thickness 11 nm is obtained after 2 h polymerization at 0.25 M monomer concentration. Thermogravimetric analysis shows the grafting amount of PNCA-F_{15} is 39.3% (2 h). Upon grafting on rough surfaces, e.g., electrochemically anodized alumina and titania, superhydrophobicity and superoleophobicity in particular can be achieved; e.g., the PNCA-F_{15} grafted rough TiO_2 nanotubes films exhibit static water contact angle of 170°.

Introduction

Synthetic polymers[1] attached to a variety of organic and inorganic substrates can provide surfaces with tunable properties such as hydrophilicity or hydrophobicity,[2] low friction,[3] corrosion and fouling resistance,[4] stimuli responsiveness,[5] and conductivity.[6] However, the major problem to be tackled is the usually weak and short-term adhesion between organic polymers and completely different materials, which is particularly true with perfluoropolymers. Considerable efforts have been focused on techniques for the preparation of well-defined polymers on solid supports. Among the available surface modification strategies, surface-initiated polymerization[7,8] (SIP) is an attractive method to form end-grafted polymer brush coatings at the nanometer scale. It not only offers control of polymer film thickness and grafting density[7−9] but also allows covalently bonding to the metal surface so as to achieve longer term stability. For SIP, an initiator is first immobilized on a surface followed by exposure of the activated surface to an appropriate polymerization solution. The vast majority of previous SIPs have utilized silane or thiol initiator to initiate polymerization from some model surfaces, for example, silicon or Au.[10] However, these initiators have limitations in modifying many other metallic substrates that is highly desirable especially for extended engineering applications. Jerome et al. have reported that electrografting is a powerful tool to attach initiator onto a number of substrates and so realize modification of substrates by subsequent SIPs,[11,12] but electrografting suffers from harsh electrochemical reaction conditions and low grafting efficiency (density). Recently, the catecholic amino acid [L-3,4-dihydroxyphenylalanine (L-DOPA)] was reported to have good adhesion onto variable metallic surfaces and SIP based on catecholic initiator reported later.[13−15] Although the adhesion mechanism is not fully understood, the good adhesion of L-DOPA has stimulated great interests in exploiting catechol for enhancing interfacial adhesion of materials.[4b,13−17]

Fluorinated polymers have many interesting properties, such as high thermal, chemical, and photochemical stability,[18] low critical surface energy,[19] and low dielectric constant.[20] The grafting of fluoropolymers makes metal surfaces become "self-cleaning" due to the polymer's excellent water- and oil-repellent properties.[21] The high stability of fluoropolymers in all environments can also provide excellent protections to metals against chemical corrosions. Fluoropolymers coatings obtained by conventional methods normally adhere to metal surfaces through van der Waals forces or other weak interactions and are prone to delamination under physical or chemical stresses. Moreover, application to nonplanar geometries will also be greatly restricted. Chemical bonding of dense perfluoropolymer films, including polymer brushes, onto solid surfaces is of great technological importance.[22−24] Generally, surface-initiated polymer films provide their fluorocarbon functionality via postprocessing methods.[25] SIP of long perfluoroalkyl chain pendant monomer is not easy even with very popular SIPs and scarcely reported. Ring-opening metathesis polymerization (ROMP) offers an effective way in polymerization of norbornene monomers with large side chain substitutes. Recently, Jennings et al. successfully employed ROMP to graft partially fluorinated polymers on gold substrates using Grubbs second generation catalyst.[26,27] In this article, we perform surface-initiated ring-opening metathesis polymerizations (SI-ROMP) of pentadecafluorooctyl-5-norbornene-2-carboxylate (NCA-F_{15}) from catecholic initiator. The good adhesion of the catecholic initiator onto variable metal substrates allows modification of these substrates with chemically bonded low surface energy polymer coatings.

*To whom correspondence should be addressed. E-mail: zhouf@lzb.ac.cn.

 Published on Web 06/10/2010

Experimental Section

Materials. 3-Hydroxytyramine hydrochloride (99%), 5-norbornene-2-carboxylic acid (97%), Grubbs first catalyst (benzylidene−bis(tricyclohexylphosphine)dichlororuthenium), and 1*H*,1*H*-perfluoro-1-octanol (98%) were used as received from Sigma-Aldrich. Dicyclohexylcarbodiimide (DCC, 98%) and 4-(dimethylamino)pyridine (DMAP, 99%) were used as received from the Chemical Reagent Co. of J&K Chemical Ltd. (Beijing, China). 1,1,2-Trichlorotrifluoroethane (99%) were used as received from Chemical Reagent Co. of Shanghai (Shanghai, China). Dichloromethane (China) was purified by distillation over CaH_2, and pyridine (China) was purified by distillation over NaOH. Ultrapure water used in all experiments was obtained from a NANOpure Infinity system from Barnstead/Thermolyne Corp. Other reagents were used as received.

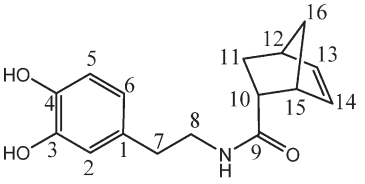

catecholic initiator

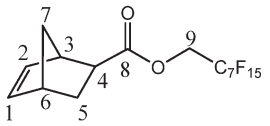

NCA-F_{15}

1. Synthesis of the Anchor Agent N-(3,4-Dihydroxyphenethyl)bicyclo[2.2.1]hept-5-ene-2-carboxamide. Dicyclohexylcarbodiimide (DCC) (2.27 g, 11 mmol) was added to a solution consisting of dopamine (1.89 g, 10 mmol), 4-(dimethylamino)-pyridine (DMAP) (61 mg, 0.5 mmol), and 5-norbornene-2-carboxylic acid (1.38 g, 10 mmol) in pyridine. The reaction mixture was stirred for 24 h at room temperature under anhydrous conditions. After evaporation under vacuum, the crude reaction product was partitioned between ethyl acetate and water. The combined organic extracts were dried over anhydrous $MgSO_4$, and the solvent was evaporated under reduced pressure to give a brown liquid. The crude product was purified by silica gel column chromatography to give colorless viscous liquid (1.77 g, 6.5 mmol, yield 65%) compound catecholic initiator (mixture of *exo* and *endo* isomers). ^{1}H NMR (400 MHz, $CDCl_3$), (ppm): major isomer (*endo*) 6.81 (dd, J = 8.0, 2.4 Hz, 1H, H-5), 6.73 (d, J = 2.0 Hz, 1H, H-2), 6.54 (dd, J = 8.0, 1.6 Hz, 1H, H-6), 6.17 (dd, J = 5.6, 3.2 Hz, 1H, H-14), 5.82 (dd, J = 5.6, 2.4 Hz, 1H, H-13), 5.64 (t, J = 5.2 Hz, 1H, N−H), 3.42 (q, J = 6.8 Hz, 2H, H-8), 3.06 (s, 1H, H-15), 2.88 (s, 1H, H-12), 2.88−2.82 (m, 1H, H-10), 2.64 (t, J = 6.8 Hz, 2H, H-7), 1.96−1.88 (m, 1H, H-11), 1.41 (dd, J = 8.4, 2.0 Hz, 1H, H-16), 1.25 (d, J = 7.2 Hz, 1H, H-11), 1.21−1.15 (m, 1H, H-16). ^{13}C NMR (100 MHz, $CDCl_3$), (ppm): 175.8 (C-9), 144.4 (C-3), 143.2 (C-4), 138.1 (C-14), 132.1 (C-13), 130.4 (C-1), 120.3 (C-2), 115.5 (C-5), 115.2 (C-6), 50.1 (C-10), 46.3 (C-15), 44.9 (C-12), 42.7 (C-8), 40.9 (C-11), 34.7 (C-7), 30.2 (C-16).

2. Synthesis of the Monomer Pentadecafluorooctyl-5-norbornene-2-carboxylate (NCA-F_{15}). A dry round-bottomed flask (100 mL) was charged with 5-norbornene-2-carboxylic acid (1.38 g; 10 mmol), 1*H*,1*H*-perfluoro-1-octanol (4.0 g, 10 mmol), dicyclohexylcarbodiimide (DCC) (2.27 g; 11 mmol), 4-(dimethylamino)pyridine (DMAP) (61 mg, 0.5 mmol), and 50 mL of dichloromethane (CH_2Cl_2). Then the reaction mixture was stirred at room temperature for 24 h. The reaction solution was extracted with CH_2Cl_2 (3 × 100 mL). The combined organic extracts were dried over anhydrous $MgSO_4$, and the solvent was evaporated under reduced pressure to give a white solid. The crude product was purified by silica gel column chromatography to give a colorless liquid (4.83 g, yield 93%) compound PNCA-F_{15} (mixture of *exo* and *endo* isomers). ^{1}H NMR (400 MHz, $CDCl_3$), (ppm): major isomer (*endo*) 6.22 (dd, J = 5.6, 3.2 Hz, 1H, H-2), 5.91 (dd, J = 5.6, 2.8 Hz, 1H, H-1), 4.61 (q, J = 13.2 Hz, 1H, H-9), 4.50 (q, J = 13.6 Hz, 1H, H-9), 3.25 (s, 1H, H-3), 3.09−3.02 (m, 1H, H-4), 2.94 (s, 1H, H-6), 1.98−1.91 (m, 1H, H-5), 1.47 (dd, J = 8.0, 2.4 Hz, 1H, H-7), 1.44−1.42 (m, 1H, H-5), 1.30 (d, J = 8.0 Hz, 1H, H-7). ^{13}C NMR (100 MHz, $CDCl_3$), (ppm): 173.2 (C-8), 138.2 (C-2), 132.0 (C-1), 59.3 (C-9), 49.7 (C-4), 45.8 (C-3), 43.0 (C-6), 42.5 (C-5), 29.1 (C-7).

3. Substrate Preparation and Modification. TiO_2 nanowires were synthesized from commercial TiO_2 granule in a Teflon-lined autoclave, as described in our previous work.[28] TiO_2 nanowires (100 mg) were immersed in a 1.6 mg/mL solution (ultrapure water:ethanol = 5:1) of initiator and stirred for 18 h in the dark at room temperature. The modified TiO_2 nanowires were isolated and purified by repeated washing with ultrapure water and ethanol using centrifugation.

4. Surface-Initiated Polymerization. In a typical SI-ROMP, 100 mg of TiO_2 nanowires modified by anchor agent (compound **1**) were immersed in a solution of 20 mg of Grubbs first catalyst in 5 mL of dichloromethane mixture, which were placed in a flask under Ar flow for 20 min. They were then carefully rinsed (three times) with pure dichloromethane using centrifugation in order to remove the excess catalyst. The [Ru]-functionalized TiO_2 nanowires (100 mg) were immersed in 5 mL of freshly prepared solutions of NCA-F_{15} (0.25 M, 0.65 g) in dichloromethane. The reaction was carried out at room temperature for 2 h. The samples were isolated from the reaction medium and extensively washed with pure dichloromethane using centrifugation. The thickness of polymer layer is about 11 nm, and the grafting about is about 0.393 g per gram of TiO_2 nanwires. The thickness of PNCA-F_{15} brush was controlled by changing polymerization time. The polymer-grafted samples were further dried under vacuum overnight before further analysis. SIP on planar substrates was performed in a similar way.

Characterization. ^{1}H (400 MHz) and ^{13}C (100 MHz) NMR was recorded on a 400 MHz spectrometer (Bruker AM-400) using $CDCl_3$ as solvent. Chemical composition information about the samples was obtained by X-ray photoelectron spectroscopy (XPS); the measurement was carried out on a PHI-5702 multifunctional spectrometer using Al Kα radiation, and the binding energies were referenced to the C 1s line at 284.8 eV from adventitious carbon. The morphology was investigated by transmission electron microscopy (TEM) (Hitachi model JEM-2010). Thermal stability was determined with a thermogravimetric analyzer (TGA) (Netzsch, STA 449 C) over a temperature range of 25−800 °C at a heating rate of 10 °C/min under a N_2 atmosphere. FT-IR was recorded on a TENSOR 27 instrument (Bruker). Scanning electron microscope (SEM) images were obtained on a JSM-6701F field-emission scanning electron microscope (FE-SEM) at 5−10 kV.

For static contact angle (CA) measurements, 5 μL of deionized water and diiodomethane (DIM, 99%, Aldrich) were chosen as the probing liquids. The contact angle measurement of a self-assembly polymer films was determined at 25 °C by contact angle goniometry using a DSA-100 optical contact-angle meter (Kruss Co., Ltd., Germany). The CAs were determined automatically using the Laplace−Young fitting algorithm. Advancing contact angle (ACA) and receding contact angle (RCA) of water droplets on the different super-repellent surfaces were measured.

Results and Discussion

Successful initiator immobilization and polymer grafting were first ascertained by XPS. Figure 1A displays the XPS full survey spectra of TiO_2 nanowires, TiO_2 nanowires modified with initiator, and those further modified with PNCA-F_{15} (2 h). The TiO_2 nanowires are mainly composed of Ti and O as well as a small amount of C resulting from adventitious hydrocarbon contamination. Successful anchoring of initiator onto TiO_2 nanowires is indicated by the presence of N signals that is not detected for the TiO_2 nanowires. The presence of the strong F 1s

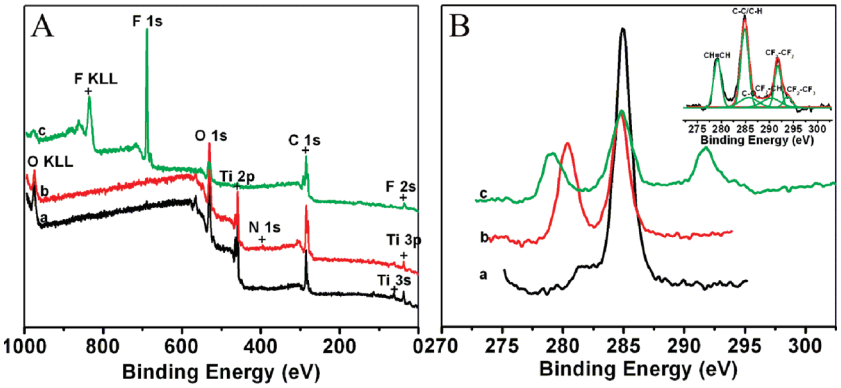

Figure 1. XPS full survey spectra (A) and C (1s) spectrum (B) of TiO_2 nanowires (a), initiator-modified TiO_2 nanowires (b), and TiO_2 nanowires−PNCA-F_{15}, (2 h) (c). The inset is the high-resolution spectrum of the C 1s region of TiO_2 nanowires−PNCA-F_{15} (2 h).

Scheme 1. Preparation of Perfluoropolymers Grafted TiO_2 Nanowires

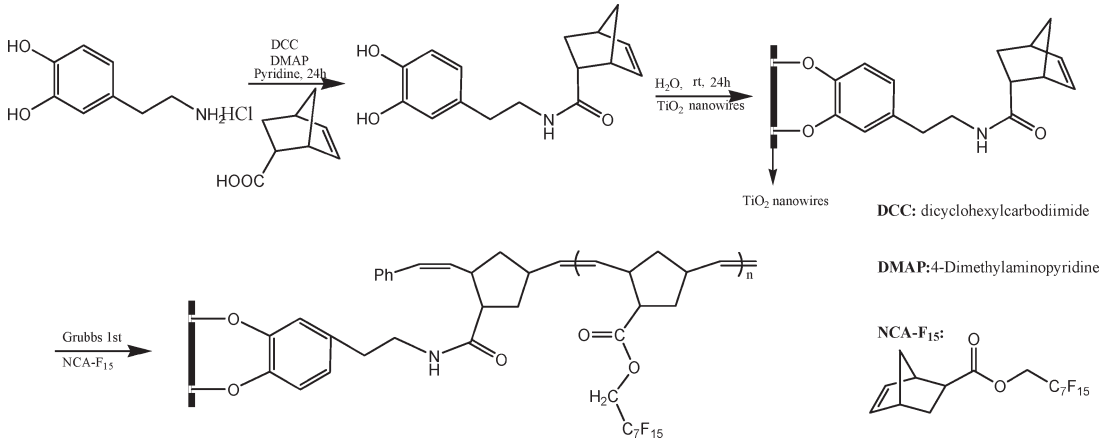

peak and C 1s peak (due to C−F) together with the C−H appearance and attenuation of the Ti 2p and Ti 2s peaks confirms that PNCA-F_{15} has been successfully grafted onto the TiO_2 nanowires surface. Compared to that of the TiO_2 nanowires, spectra of the sample after PNCA-F_{15} modification (inset of Figure 1B) consist of six components centered at binding energies of 279.2, 284.8, 285.8, 290.5, 291.6, and 293.9 eV, corresponding to C=C, C−C, C−O, CF_2−CH_2, CF_2−CF_2, and CF_3−CF_2 groups, respectively. This is in good agreement with the results reported.[29] Another obvious characteristic of the presence of PNCA-F_{15} brushes is the large-intensity peaks of the F 1s peak at 689.0 eV. The main peak corresponding to CF_x indicates that the PNCA-F_{15} coating is on the outermost surface, while the F 1s peak of metal fluoride located at 684.4 eV.[30]

Figure 2 demonstrates the FT-IR spectrum evolution from blank TiO_2, to initiator-modified TiO_2 to polymer-grafted TiO_2 after 2 h. Blank TiO_2 shows a featureless spectrum except for the wide absorption peaks of absorbed water above 3000 cm^{-1}. Typical features of the PNCA-F_{15} backbone include a sharp absorptions peak at 1751 cm^{-1} from C=O stretch in the ester group; the IR spectrum for PNCA-F_{15} exhibits absorbance peaks for perpendicular C−F stretching modes at 1246, 1210, and 1149 cm^{-1}. The CF_2 stretching modes absorb strongly from 1100 to 1400 cm^{-1}. Because of the helical structure of fluoroalkyl chains, two types of CF_2 stretching peaks are expected in the IR: those lying along the helical axis ($\nu_{ax}(CF_2)$, 1300−1400 cm^{-1}) and those perpendicular to the helical axis ($\nu_{pd}(CF_2)$, 1100−1300 cm^{-1}).[31,32] The ratio of $\nu_{pd}(CF_2)$ to $\nu_{ax}(CF_2)$ absorbance for PNCA-F_{15}−TiO_2 nanowires provides information on the orientation of the fluorocarbon side chains in the polymer film relative

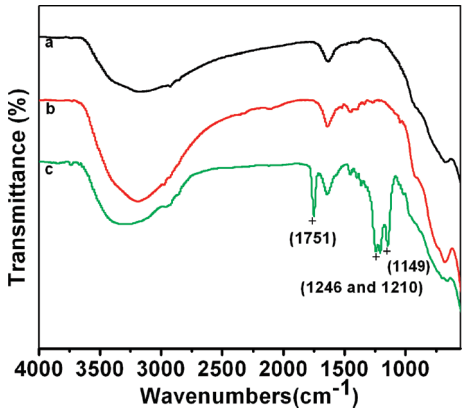

Figure 2. FT-IR spectra of (a) TiO_2 nanowires, (b) TiO_2 nanowires-initiator modified, and (c) TiO_2 nanowires−PNCA-F_{15} (2 h).

to the surface normal due to IR inherent surface selection.[33] When $\nu_{pd}(CF_2)$ to $\nu_{ax}(CF_2)$ is ≫1, the fluorocarbon chains are generally oriented parallel to the surface; if $\nu_{pd}(CF_2)$ to $\nu_{ax}(CF_2)$ is ≪1, the fluorocarbon chains are primarily oriented normal to the surface.[33] We observe a high ratio of $\nu_{pd}(CF_2)$ to $\nu_{ax}(CF_2)$ absorbance (≫1) in the surface-grafted PNCA-F_{15}, as shown in Figure 2C, indicating the fluorinated side chains of the polymer are generally oriented more along the parallel to the TiO_2 nanowires substrate. This parallel orientation of the fluorocarbon groups is similar to a previous report.[25,26]

TGA were carried out in order to evaluate the change of organic portion during polymer grafting on the TiO_2 nanowires at different monomer concentrations and set polymerization time

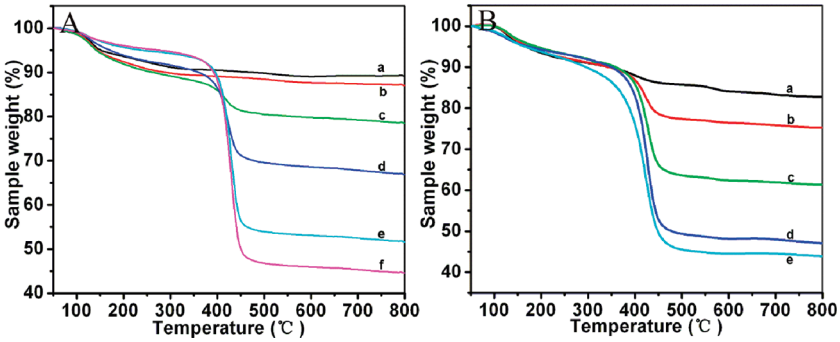

Figure 3. (A) TGA traces of TiO_2 nanowires (a), TiO_2 nanowires-initiator modified (b), TiO_2 nanowires−PNCA-F_{15}, (0.05 M, 2 h) (c), TiO_2 nanowires−PNCA-F_{15}, (0.1 M, 2 h) (d), TiO_2 nanowires−PNCA-F_{15}, (0.25 M, 2 h) (e), and TiO_2 nanowires−PNCA-F_{15}, (0.5 M, 2 h) (f). (B) TGA curves of TiO_2 nanowires−PNCA-F_{15}, (0.25 M, 15 min) (a), TiO_2 nanowires−PNCA-F_{15}, (0.25 M, 30 min) (b), TiO_2 nanowires−PNCA-F_{15}, (0.25 M, 1 h) (c), TiO_2 nanowires−PNCA-F_{15}, (0.25 M, 2 h) (d), and TiO_2 nanowires−PNCA-F_{15}, (0.25 M, 4 h) (e).

Table 1. Surface Analysis Results of Initiator-Modified TiO_2 Nanowires and Polymer-Grafted TiO_2 Nanowires (Different Polymerization Time SI-ROMP) Samples

	XPS atomic concentration (%)				
sample	[O]	[Ti]	[N]	[C]	[F]
initiator-modified TiO_2	29.22	7.76	0.64	62.38	0
TiO_2-*g*-PNCAF_{15}-1[a]	22.80	6.02	0	42.58	28.59
TiO_2-*g*-PNCAF_{15}-2[b]	19.87	3.13	0	42.42	34.57
TiO_2-*g*-PNCAF_{15}-3[c]	18.23	1.82	0	43.12	36.84
TiO_2-*g*-PNCAF_{15}-4[d]	14.08	0.39	0	45.21	40.31

[a] Polymerization time = 15 min. [b] Polymerization time = 30 min. [c] Polymerization time = 1 h. [d] Polymerization time = 2 h.

or at different polymerization time. As seen in Figure 3A, very similar one-step degradation profiles for TiO_2 nanowires−PNCA-F_{15} samples were observed. For instance, a typical graft polymer sample (TiO_2 nanowires−PNCA-F_{15}, 2 h polymerization) exhibited one thermal decomposition processes about 400 °C, which shows that grafted polymer (PNCA-F_{15}) has good temperature stability. TGA of TiO_2 nanowires measured 9.5% weight loss between 100 and 600 °C. Upon modification of ROMP initiator, the composite was found to have 11.0% weight loss, so 1.5 wt % of the composite was ROMP initiator. TGA traces show the change of organic portion during polymer grafting on the TiO_2 nanowires at different concentrations and 2 h set polymerization time (Figure 3A). TGA provided evidence for the systematic increase in the amount of PNCA-F_{15} with the monomer concentrations. After polymerization through ROMP, the samples have 18.8% (0.05 M), 30.6% (0.1 M), 46.2% (0.25 M), and 53.2% (0.5 M) weight loss between 100 and 600 °C. A similar TGA profile was also observed for grafted samples with the different polymerization time (Figure 3B). According to TGA result of TiO_2 nanowires−PNCA-F_{15} (0.25 M) at the different polymerization time, the residual mass percent is 84.1% (15 min), 76.5% (30 min), 62.4% (1 h) 48.2% (2 h), and 44.5% (4 h) at 600 °C, which shows the grafting amount of PNCA-F_{15} is 4.8% (15 min), 12.6% (30 min), 26.6% (1 h), 39.3% (2 h), and 43.2% (4 h) after deduction of initiator contribution. Polymer grafting levels off after 2 h. XPS provides evidence for the systematic increase in the amount of PNCA-F_{15} with the polymerization time, and the surface chemical composition data of these surfaces together with initiator-modified TiO_2 are summarized in Table 1. It is seen that O, Ti, and N are gradually attenuated by grafting of polymer, concurrent with the significantly increased fluorine extent.

The presence of polymer layer was further verified by TEM characterization. The PNCA-F_{15}−TiO_2 nanowires (2 h) sample was prepared by dropping their dispersion in 1,1,2-trichlorotrifluoroethane onto a carbon-coated copper grid. Nongrafted TiO_2 nanowires were all aggregates of 20 to over 100 nm. In contrast,

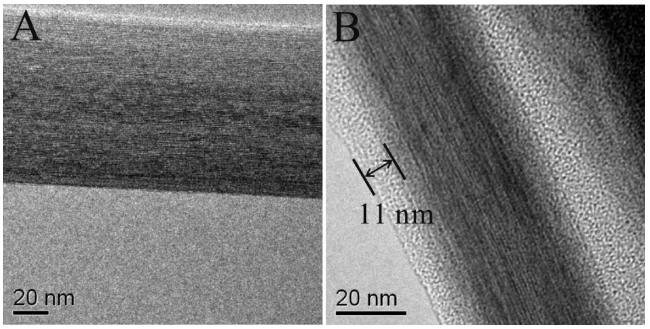

Figure 4. TEM images of TiO_2 nanowires (A) and PNCA-F_{15}−TiO_2 nanowires (2 h).

PNCA-F_{15}-grafted−TiO_2 nanowires were observed to have fine dispersivity of separate wires, and no obvious aggregation was found (image not shown). These findings clearly revealed that the PNCA-F_{15}−TiO_2 nanowires allow dispersion and stability in appropriate solvents. Figure 4 shows high-resolution transmission electron microscopic (HRTEM) images of nongrafted TiO_2 nanowires and surface morphology of PNCA-F_{15}-*g*-TiO_2 nanowires (2 h). From Figure 4A, one can see relatively clear crystalline orientation of TiO_2 nanowires. All the PNCA-F_{15}-*g*-TiO_2 nanowires are homogeneously coated with a very uniform layer, and the interface boundary is very clear (Figure 4B). It is seen that the PNCA-F_{15} layer has a lighter color than the sidewall of TiO_2 nanowires due to lower density. Increasing polymerization time, the thickness of surface coatings increases with time (data not shown). After TiO_2 nanowires−PNCA-F_{15} (2 h) was formed, the shell thickness increased to 11 nm (Figure 4B) compared with TiO_2 nanowires (Figure 4A). The polymer coatings reported here are significantly thicker than those formed by adsorption of DOPA-functionalized polymers from solution ("graft-to" approach) onto similar substrates.[34] The interaction is likely to take the form of a bidentate coordination complex between the catechol oxygens and a TiO_2 nanowires surface.[35] Binding energies between TiO_2 and dopamine have recently been estimated by density functional theory to be on the order of 25−30 kcal/mol,[36] suggesting that grafted polymer chains are strongly bound to the TiO_2 nanowires surface.

Because of the strong adhesion of the catechol group, growing hydrophobic polymer brushes (PNCA-F_{15}) onto variable metal surfaces is possible. All metal substrates were subsequently cleaned by ultrasonication in the following media: ultrapure water, acetone, petroleum ether, and 2-propanol. The substrates were further cleaned in an oxygen plasma chamber (Harrick Scientific) at < 200 mTorr and 100 W for 10 min. After O_2 plasma and initiator adsorption procedures, substrates were subjected to

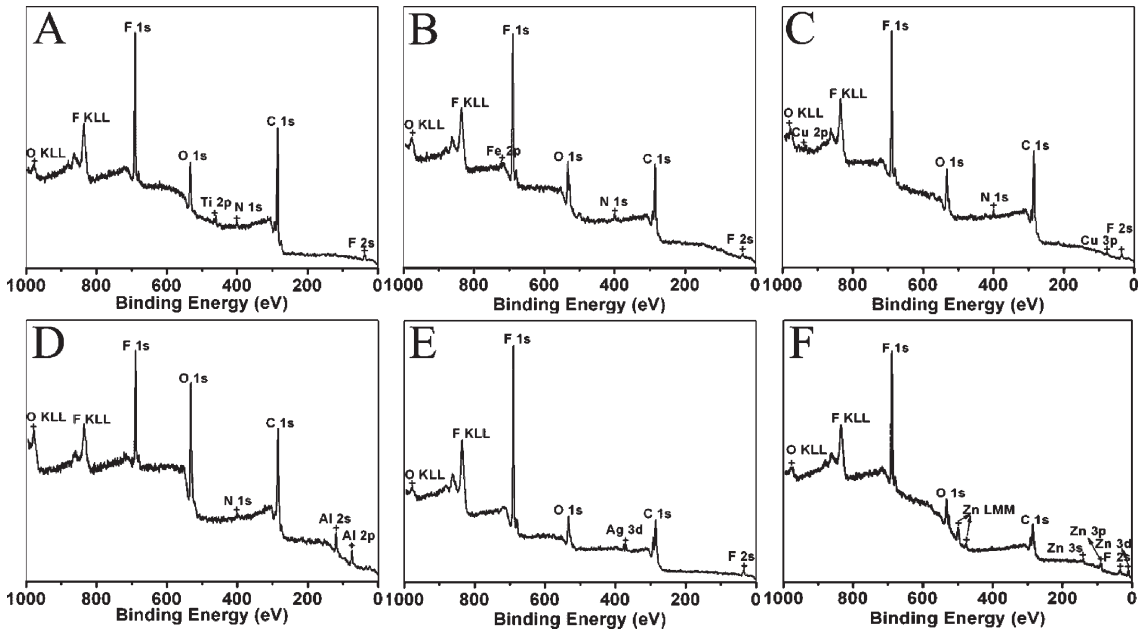

Figure 5. XPS survey spectra of PNCA-F_{15}−Ti (A), PNCA-F_{15}−Fe (B) PNCA-F_{15}−Cu (C), PNCA-F_{15}−Al (D), PNCA-F_{15}−Ag (E), and PNCA-F_{15}−Zn (F).

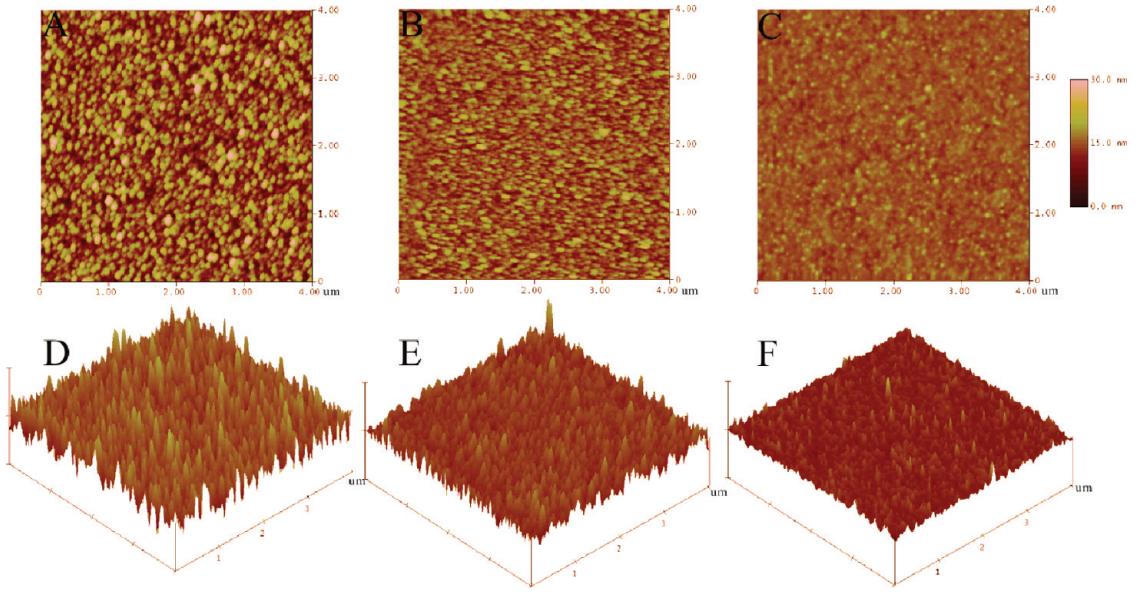

Figure 6. 4 × 4 μm AFM images of Ti (titanium was deposited on silicon wafer) before (A) and after (B) (30 min), (C) (2 h) modification of polymer brush. (D), (E), and (F) show 3D rendered version on the same *z*-scale (30 nm).

SI-ROMP in the absence of 0.5 M monomer PNCA-F_{15} for 30 min. The polymer-grafted samples were further dried under vacuum overnight before further analysis. Figure 5 displays the XPS survey spectra of PNCA-F_{15}−Cu, PNCA-F_{15}−Ag, PNCA-F_{15}−Fe, PNCA-F_{15}−Zn, PNCA-F_{15}−Al, and PNCA-F_{15}−Ti. Successful polymer grafting was ascertained by XPS through the presence of F signals, which demonstrate good adhesion between a catechol-based initiator and native metal substrates. To check the surface morphology and the thickness of the poly(PNCA-F_{15}) brushes grown on the titanium surface (100 nm Ti on Si wafers), AFM measurements were performed. Figure 6 shows the 4.0 μm × 4.0 μm tapping-mode AFM phase images of Ti and PNCA-F_{15}−Ti. Before modification (Figure 6A), small particles, about 60−180 nm grain size, height ranges from 5 to 30 nm, are seen uniformly distributed over the whole surface of Ti. After 30 min polymerization onto Ti surface (Figure 6B), the roughness of the surface of Ti polymer (PNCA-F_{15}) became small, which is apparently due to polymer brush modification. After 2 h polymerization time, large grains disappeared over the surface; the rms roughness also decreased from 4.9 to 1.3 nm.

Application of the polymer grafting strategy was tested by modification of Al and TiO_2 with microscale and also nanostructures and thus resultant extreme wettability (Figures 7 and 8). Figure 7 shows the XPS and FESEM images of resultant alumina nanowires[37] and TiO_2 nanotubes[38] films. It is seen that grafting several to over 10 nm thick polymer film does not mask the nanostructure (alumina nanowires and TiO_2 nanotubes), which is key in enhancing the hydrophobicity. Figure 8 summarizes the advancing contact angle values of water and CH_2I_2 droplets in contact with PNCA-F_{15} on the different rough surfaces. A water droplet of 5 μL exhibits a typical spherical shape on alumina (Figure 8A) with CA of over 160° (ACA = 165°, RCA = 163°)

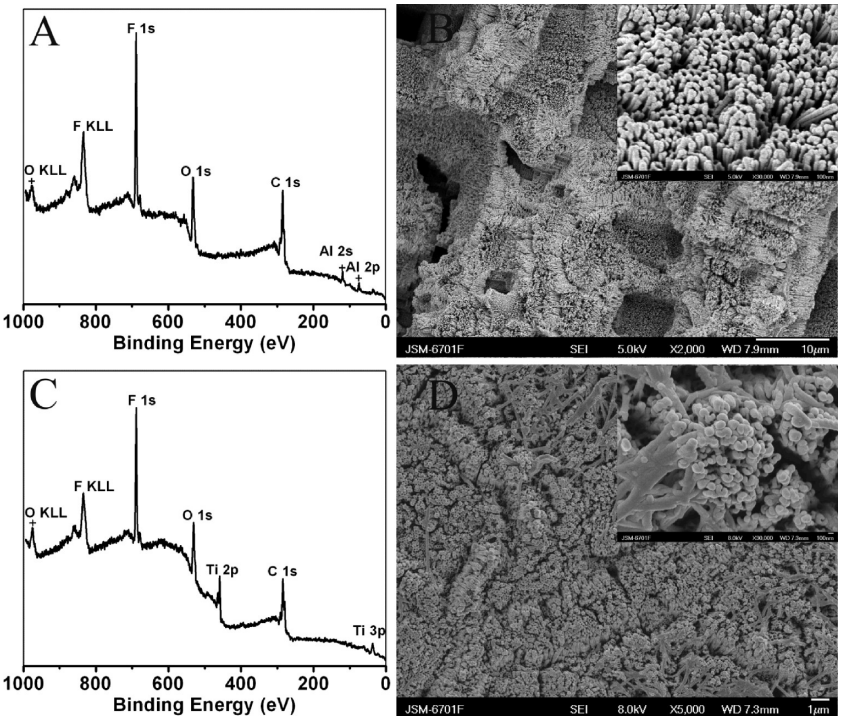

Figure 7. XPS survey spectra (A) and SEM images (B) of PNCA-F_{15}−alumina nanowires and that of PNCA-F_{15}−TiO_2 nanotubes (C, D).

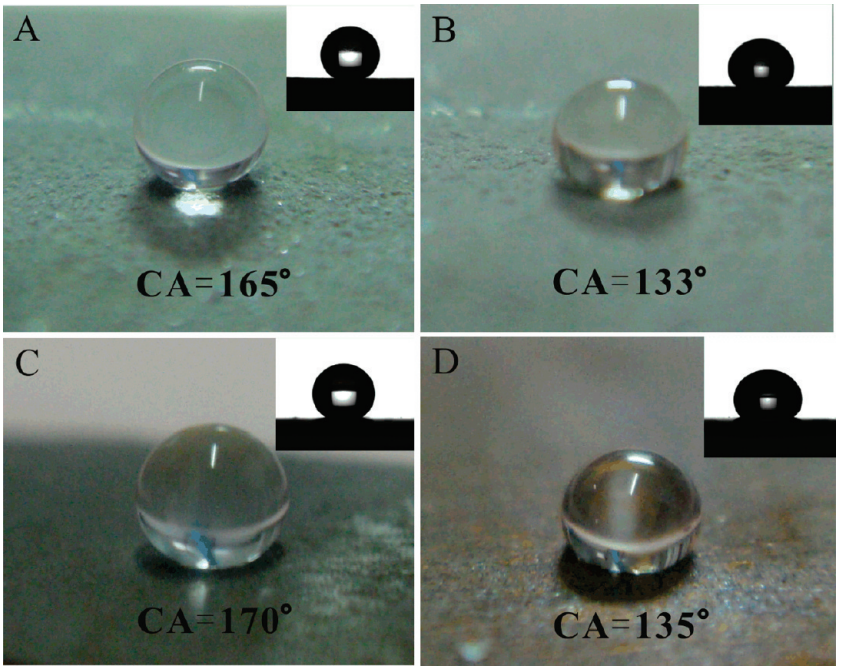

Figure 8. Photos and contact angles of representative static liquid droplets with different surface tensions on the different super-repellent surfaces. PNCA-F_{15}−alumina nanowires: (A) water, (B) diiodomethane. PNCA-F_{15}−TiO_2 nanotubes: (C) water, (D) diiodomethane.

and easily rolls off at the tilting angle of 2°. The surface displays super-repellency toward CH_2I_2 (Figure 8B); similar super-repellency was found for alkane liquids such as hexadecane, the CA of which are all above 141°. The water CA of the PNCA-F_{15} fluorinated rough TiO_2 nanotubes films is about 170° (ACA = 171°, RCA = 166°),[39] with a small sliding angle under measurement (2°). Clearly, the surface is close to the pure Cassie model, in which a high air fraction on the surface enables easy sliding of droplets and very low contact angle hysteresis. The surface displays repellency toward CH_2I_2, the CA of which is 135°. The fluorinated samples surface is fully covered with a fluorine polymer, with the $-CF_3$ terminal groups orientated outside together with a high air fraction, making the samples superhydrophobic and nonadhesive.

Conclusions

In this work, we have demonstrated for the first time the surface-initiated ring-opening metathesis polymerization from catechol-based initiator. The assembly capability of the initiator on variable metals and metallic oxides allows modification of these substrates with, for example, the low surface energy perfluoroalkyl-substituted polymer brushes in the present work. The

grafting polymerizations were well behaved and readily controlled, and the resultant thickness of polymer is in the range of 10−15 nm. The approach combines the advantages of catecholic initiator with SI-ROMP to grow good adhesion and thermally stable films under ambient conditions. A suitable rough substrate (alumina nanowires and TiO_2 nanotubes) upon modification with low surface energy fluoropolymer brushes turns to superrepellent toward liquids, such as water and some oils.

Acknowledgment. The work is financially supported by "Top Hundred Talents" Program of CAS and Key Project of NSFC (50835009, 20973188) and "973" (2007CB607601).

References and Notes

(1) (a) Place, E. S.; George, J. H.; Williams, C. K.; Stevens, M. M. *Chem. Soc. Rev.* **2009**, *38*, 1139–1151. (b) Percec, V. *Chem. Rev.* **2009**, *109*, 4961–4962.
(2) Zou, Y. Q.; Rossi, N. A. A.; Kizhakkedathu, J. N.; Brooks, D. E. *Macromolecules* **2009**, *42*, 4817–4828.
(3) (a) Gill, L.; Damron, J.; Wachowicz, M.; White, J. L. *Macromolecules* **2010**, *43*, 3903–3910. (b) Nordgren, N.; Rutland, M. W. *Nano Lett.* **2009**, *9*, 2984–2990.
(4) (a) Yuan, S. J.; Pehkonen, S. O.; Ting, Y. P.; Neoh, K. G.; Kang, E. T. *Langmuir* **2010**, *26*, 6728–6736. (b) Saxer, S.; Portmann, C.; Tosatti, S.; Gademann, K.; Zurcher, S.; Textor, M. *Macromolecules* **2010**, *43*, 1050–1060.
(5) (a) Matsumoto, S.; Christie, R. J.; Nishiyama, N.; Miyata, K.; Ishii, A.; Oba, M.; Koyama, H.; Yamasaki, Y.; Kataoka, K. *Biomacromolecules* **2009**, *10*, 119–127. (b) Yu, L.; Ding, J. D. *Chem. Soc. Rev.* **2008**, *37*, 1473–1481.
(6) (a) Miyazaki, S.; Endo, H.; Karino, T.; Haraguchi, K.; Shibayama, M. *Macromolecules* **2007**, *40*, 4287–4295. (b) Haraguchi, K.; Li, H. J. *Macromolecules* **2006**, *39*, 1898–1905.
(7) Barbey, R.; Lavanant, L.; Paripovic, D.; Schuwer, N.; Sugnaux, C.; Tugulu, S.; Klok, H. A. *Chem. Rev.* **2009**, *109*, 5437–5527.
(8) (a) Edmondson, S.; Osborne, V. L.; Huck, W. T. S. *Chem. Soc. Rev.* **2004**, *33*, 14–22. (b) Azzaroni, O.; Zheng, Z. J.; Yang, Z. Q.; Huck, W. T. S. *Langmuir* **2006**, *22*, 6730–6733. (c) Azzaroni, O.; Brown, A. A.; Cheng, N.; Wei, A.; Jonas, A. M.; Huck, W. T. S. *J. Mater. Chem.* **2007**, *17*, 3433–3439.
(9) (a) Zhao, B.; Brittain, W. J. *Prog. Polym. Sci.* **2000**, *25*, 677–710. (b) Jennings, G. K.; Brantley, E. L. *Adv. Mater.* **2004**, *16*, 1983–1994.
(10) Pyun, J.; Kowalewski, T.; Matyjaszewski, K. *Macromol. Rapid Commun.* **2003**, *24*, 1043–1059.
(11) (a) Ignatova, M.; Voccia, S.; Gilbert, B.; Markova, N.; Cossement, D.; Gouttebaron, R.; Jerome, R.; Jerome, C. *Langmuir* **2006**, *22*, 255–262. (b) Ignatova, M.; Voccia, S.; Gabriel, S.; Gilbert, B.; Cossement, D.; Jerome, R.; Jerome, C. *Langmuir* **2009**, *25*, 891–902.
(12) (a) Jerome, C.; Jerome, R. *ACS Symp. Ser.* **2005**, *912*, 84–104. (b) Claes, M.; Voccia, S.; Detrembleur, C.; Jerome, C.; Gilbert, B.; Leclere, P.; Geskin, V. M.; Gouttebaron, R.; Hecq, M.; Lazzaroni, R.; Jerome, R. *Macromolecules* **2003**, *36*, 5926–5933. (C) Detrembleur, C.; Jerome, C.; Claes, M.; Louette, P.; Jerome, R. *Angew. Chem., Int. Ed.* **2001**, *40*, 1268–1271.
(13) Fan, X. W.; Lin, L. J.; Dalsin, J. L.; Messersmith, P. B. *J. Am. Chem. Soc.* **2005**, *127*, 15843–15847.
(14) Ye, Q.; Wang, X. L.; Hu, H. Y.; Wang, D. A.; Li, S. B.; Zhou, F. *J. Phys. Chem. C* **2009**, *113*, 7677–7683.
(15) (a) Dalsin, J.; Tosatti, S.; Voros, J.; Textor, M.; Messersmith, P. B. *Langmuir* **2005**, *21*, 640–646. (b) Statz, A. R.; Meagher, R. J.; Barron, A. E.; Messersmith, P. B. *J. Am. Chem. Soc.* **2005**, *127*, 7972–7973. (c) Dalsin, J. L.; Hu, B.-H.; Lee, B. P.; Messersmith, P. B. *J. Am. Chem. Soc.* **2003**, *125*, 4253–4258.
(16) Yu, M.; Deming, T. J. *Macromolecules* **1998**, *31*, 4739–4745.
(17) Malisova, B.; Tosatti, S.; Textor, M.; Gademann, K.; Zurcher, S. *Langmuir* **2010**, *26*, 4018–4026.
(18) Garbassi, F.; Morra, M.; Occhiello, E. *Polymer Surfaces: From Physics to Technology*; John Wiley & Sons: Chichester, 1998.
(19) Wang, J. G.; Mao, G. P.; Ober, C. K.; Kramer, E. J. *Macromolecules* **1997**, *30*, 1906–1914.
(20) Rutenberg, I. M.; Scherman, O. A.; Grubbs, R. H.; Jiang, W.; Garfunkel, E.; Bao, Z. *J. Am. Chem. Soc.* **2004**, *126*, 4062–4063.
(21) Granville, A. M.; Brittain, W. J. *Macromol. Rapid Commun.* **2005**, *38*, 2137–2142.
(22) (a) Chang, Y. C.; Franck, C. W. *Langmuir* **1998**, *14*, 326–334. (b) Hyun, J.; Chilkoti, A. *Macromolecules* **2001**, *34*, 5644–5652.
(23) (a) Huseman, M.; Morrison, M.; Benoit, D.; Frommer, J.; Mate, C. M.; Hinsberg, W. D.; Hedrick, J. L.; Hawker, C. J. *J. Am. Chem. Soc.* **2000**, *122*, 1844–1845. (b) Jordan, R.; West, N.; Ulman, A.; Chou, Y. M.; Nuyken, O. *Macromolecules* **2001**, *34*, 1606–1611.
(24) (a) Prucker, O.; Naumann, C. A.; Ruhe, J.; Knoll, W.; Frank, C. W. *J. Am. Chem. Soc.* **1999**, *121*, 8766–8770. (b) Quirk, R. P.; Mathers, R. T. *Polym. Bull.* **2001**, *45*, 471–477.
(25) Brantley, E. L.; Jennings, G. K. *Macromolecules* **2004**, *37*, 1476–1483.
(26) Faulkner, C. J.; Fischer, R. E.; Jennings, G. K. *Macromolecules* **2010**, *43*, 1203–1209.
(27) Berron, B.; Faulkner, C. J.; Fischer, R. E.; Payne, P. A.; Jennings, G. K. *Langmuir* **2009**, *25*, 12721–12728.
(28) Wang, D. A.; Zhou, F.; Wang, C. W.; Liu, W. M. *Microporous Mesoporous Mater.* **2008**, *116*, 658–664.
(29) (a) Lai, Y, K.; Lin, C. J.; Huang, J. Y.; Zhuang, H. F.; Sun, L.; Nguyen, T. *Langmuir* **2008**, *24*, 3867–3873. (b) Hozumi, A.; Ushiyama, K.; Sugimura, H.; Takai, O. *Langmuir* **1999**, *15*, 7600–7604.
(30) Macak, J. M.; Aldabergerova, S.; Ghicov, A.; Schmuki, P. *Phys. Status Solidi A* **2006**, *203*, R67–R69.
(31) Genzer, J.; Sivaniah, E.; Kramer, E. J.; Wang, J. G.; Korner, H.; Xiang, M. L.; Char, K.; Ober, C. K.; DeKoven, B. M.; Bubeck, R. A.; Chaudhury, M. K.; Sambasivan, S.; Fischer, D. A. *Macromolecules* **2000**, *33*, 1882–1887.
(32) Seehof, N.; Grutke, S.; Risse, W. *Macromolecules* **1993**, *26*, 695–700.
(33) Parikh, A. N.; Allara, D. L. *J. Chem. Phys.* **1992**, *96*, 927–945.
(34) (a) Zorn, M.; Meuer, S.; Tahir, M. N.; Khalavka, Y.; Sönnichsen, C.; Tremel, W.; Zentel, R. *J. Mater. Chem.* **2008**, *18*, 3050–3058. (b) Tahir, M. N.; Eberhardt, M.; Theato, P.; Faiss, S.; Janshoff, A.; Gorelik, T.; Kolb, U.; Tremel, W. *Angew. Chem., Int. Ed.* **2006**, *45*, 908–912.
(35) (a) Connor, P. A.; Dobson, K. D.; McQuillan, A. J. *Langmuir* **1995**, *11*, 4193–4195. (b) Rajh, T.; Chen, L. X.; Lukas, K.; Liu, T.; Thurnauer, M. C.; Tiede, D. M. *J. Phys. Chem. B* **2002**, *106*, 10543–10552.
(36) Vega-Arroyo, M.; LeBreton, P. R.; Rajh, T.; Zapol, P.; Curtiss, L. A. *Chem. Phys. Lett.* **2005**, *406*, 306–311.
(37) Wu, W.; Wang, X.; Wang, D.; Chen, M.; Zhou, F.; Liu, W.; Xue, Q. *Chem. Commun.* **2009**, 1043–1045.
(38) Wang, D.; Liu, Y.; Yu, B.; Zhou, F.; Liu, W. *Chem. Mater.* **2009**, *21*, 1198–1206.
(39) Cassie, A. B. D.; Baxter, S. *Trans. Faraday Soc.* **1944**, *40*, 546–561.